Eur. Phys. J. B **17**, 85–94 (2000)

THE EUROPEAN PHYSICAL JOURNAL B

EDP Sciences

On electron pairing in unconventional superconductors

P. Brovetto[a], V. Maxia, and M. Salis

Istituto Nazionale di Fisica della Materia, 09124 Cagliari, Italy
and
Istituto di Fisica Superiore dell'Università di Cagliari, Via Ospedale 72, 09124 Cagliari, Italy

Received 3 November 1999 and Received in final form 18 May 2000

Abstract. This paper presents a study whose aim is to decide whether the basic mechanism of electron pairing is the same for all unconventional superconductors such as perovskites, cuprates, organic compounds and alkaly-stuffed fullerene. By analyzing the features of these dissimilar materials, arguments are singled out showing that superconduction is originated by electrons combined in weakly bound pairs running in regions bordering on certain lattice discontinuities which are common to the structure of the superconductors dealt with. Special attention is devoted to the properties of the YBCO cuprate.

PACS. 74.20.-z Theories and models of superconducting state

1 Introduction

Till now, no definitive explanation has been found for high T_c superconduction in cuprates [1]. The most accredited opinion is that superconduction in these materials arises from singlet electron pairs as in the BCS theory, but with a pairing mechanism different and more effective than electron-phonon coupling. Such a mechanism should convert the electron-lattice interaction into a binding force that stabilizes the pairs which are thus allowed to move freely through the lattice as do Cooper's pairs. According to BCS theory, the superconducting ground state is separated from the lowest excited state by an energy gap of amplitude depending on binding force strength [2]. This result follows directly from the Bogolyubov-Valatin (BV) transformation, which shows that an interacting electron system is equivalent to a set of non-interacting quasiparticles [3,4]. The BV transformation is quite general and can be applied to different fermion systems independently of the actual pairing mechanism. As a consequence, if a suitable pairing mechanism is singled out, the outcome of BCS theory, that is, the existence of a gap, the critical temperature-gap amplitude relationship, the intrinsic coherence length and so on, remain valid for cuprates as well.

Cuprates surely represent the most interesting superconductors as they show the highest T_c so far recorded. But various unconventional superconductors other than cuprates are known. Although these materials show low critical temperatures, they are worthy of consideration because their peculiarities may supply data useful in finding a general explanation of the electron pairing mechanism suitable for all unconventional superconductors. Table 1 below gives a short list of the superconductors dealt with.

Actually, superconduction has been observed since 1964 in reduced strontium titanate, $SrTiO_{3-\delta}$, but at quite low temperatures, that is 0.25 - 0.28 K [5]. In 1975, the mixed oxide $BaPb_{0.7}Bi_{0.3}O_3$ showing 13 K superconduction was singled out [6]. After the discovery of cuprates in 1986 [7], superconduction was detected at 30 K in the $Ba_{0.6}K_{0.4}BiO_3$ compound [8]. Recently, an analogous result was reached with $Sr_{1-x}K_xBiO_3$ (x = 0.45 - 0.6) and $Sr_{0.5}Rb_{0.5}BiO_3$ compounds, which superconduct at about 12 K and 13 K, respectively [9]. Organic superconductors are quite different materials. Let us mention, in this connection, the Bechgaard salt, that is, tetramethyl-tetraselena-fulvalene hexafluorophosphate $(TMTSF)_2PF_6$, which superconducts at about 1 K [10]. But the most striking case is that of alkali-stuffed fullerene. With K_xC_{60} and Rb_xC_{60} ($x \leq 3$), superconduction was observed at 18 K and 28 K, respectively [11]. Of course, the previous list of superconductors is completed with cuprates. On the whole, the superconductors mentioned in Table 1 can be divided into four groups, that is, 1 - 5 perovskites, 6 organic compounds, 7 - 8 fullerenes, 9 - 10 cuprates. Therefore, four kinds of superconduction mechanisms should be considered in principle. It is obvious, however, that a unitary explanation is preferable. It is to be searched for in something that is common to all materials notwithstanding their very different natures. For this reason, some special features of the superconductors dealt with are now examined.

2 Features common to unconventional superconductors

2.1 Electronic configuration

Let us first consider the electronic configurations of atoms and ions sharing in the material compositions. The reduced strontium titanate cell consists of a perovskitic cube

[a] e-mail: brovetto@vaxcal.unica.it

Table 1. Some unconventional superconductors.

	Superconductor	T_c (K)	Electronic configuration	Structure
1	$SrTiO_{3-\delta}$	0.28	$Ti^{+3} \rightarrow [Ar]\,3d^1$	Dishomogeneous perovskite
2	$BaPb_{0.7}Bi_{0.3}O_3$	13	$Bi^{+4} \rightarrow [Xe]\,4f^{14}5d^{10}6s^1$	"
3	$Ba_{0.6}K_{0.4}BiO_3$	30	"	"
4	$Sr_{0.5}K_{0.5}BiO_3$	12	"	"
5	$Sr_{0.5}Rb_{0.5}BiO_3$	13	"	"
6	$(TMTSF)_2PF_6$	~ 1	$(TMTSF)^{+1}$ free radical	Molecular stackings
7	K_xC_{60}	18	$K \rightarrow [Ar]\,4s^1$	Stacking of C_{60} spheres
8	Rb_xC_{60}	28	$Rb \rightarrow [Kr]\,5s^1$	"
9	La_2CuO_4	35	$Cu^{+2} \rightarrow [Ar]\,3d^9$	Layered (K_2NiF_4)
10	$YBa_2Cu_3O_7$	92	"	Layered perovskite

with a strontium ion at the centre. The Ti^{+4} ions at the cube vertices show the [Ar] configuration, but, owing to the partial lack of oxygen, a number of Ti^{+3} ions with the $[Ar]\,3d$ configuration, showing an excess $3d$-electron, is present as well. This means that unpaired electrons are found in some cells. In the mixed perovskitic oxide $BaPb_{0.7}Bi_{0.3}O_3$, bismuth is forced to assume valence four like lead. But, while Pb^{+4} ions show the $[Xe]\,4f^{14}5d^{10}$ configuration, Bi^{+4} ions show the $[Xe]\,4f^{14}5d^{10}6s$ configuration, in which an unpaired $6s$-electron is present. Analogous arguments apply to $Ba_{0.6}K_{0.4}BiO_3$ oxide in which 60% of bismuth ions are tetravalent. The situation is quite similar for compounds with the barium-strontium and potassium-rubidium substitutions, which again hold tetravalent bismuth. Unpaired electrons are found in all these perovskitic oxides. In the Bechgaard salt one electron is transferred from one TMTSF molecule to one fluorine atom so that $(TMTSF)^{+1}$ cations and $(PF_6)^{-1}$ anions appear. Since in neutral TMTSF molecules all electrons are coupled in $\sigma-$ or $\pi-$bonds, one unpaired electron is present in the $(TMTSF)^{+1}$ cation, which consequently behaves as a free radical. In the alkaly stuffed fullerene, unpaired electrons are inserted in the material by the alkaly atoms themselves. Potassium and rubidium are in fact characterized by the $[Ar]\,4s$ and $[Kr]\,5s$ configurations showing unpaired $4s$- and $5s$-electrons, respectively. Cuprates consist of a wide variety of metal oxides in which copper is kept in perovskitic structures. For brevity's sake, we will consider only the first compound discovered, La_2CuO_4 [7] and the YBCO cuprate, $YBa_2Cu_3O_7$, which is perhaps the most representative material. Their stoichiometry includes divalent copper showing the $[Ar]\,3d^9$ configuration in which an unpaired electron is found in a half-filled $3d$-state. The conclusion follows that the presence of unpaired electrons is indeed a feature common to all materials considered up to now. What is more, inert compounds, such as $BaPbO_3$ and C_{60}, become superconductors when treated in such a way that unpaired electrons appear in them.

2.2 Structure

But another notable feature equalises these materials. All show uneven lattices with a blend of cells of different stoichiometries or with complex anisotropic cells. Actually, a fractional cell stoichiometry is common to all the perovskitic oxides mentioned previously, that is, $SrTiO_{3-\delta}$, $BaPb_{0.7}Bi_{0.3}O_3$ and so on. In Bechgaard salt we find stackings of strongly bound molecules with a much weaker intermolecular bonding in directions transverse to the stackings. Alkaly stuffed fullerene, in turn, shows a stack of C_{60} balls in which links between carbons in contiguous balls are weaker than links between carbons in the same ball. As for cuprates, the La_2CuO_4 compound shows a layered structure like that of K_2NiF_4, while YBCO is characterized by a layered structure showing couples of contiguous CuO_2 planes intercalated with barium-centred perovskitic cubes. It follows that the presence of faults in structure continuity is indeed a feature common to all the superconductors considered above. In reality, leaving metallic solids aside, no superconductor showing a simple regular lattice is known. Let us mention, in this connection, the divalent copper oxide which is characterized by a monoclinic lattice (S.G. C12/c1, monoclinic no. 15). This material, which can be regarded as the simplest cuprate, is not a superconductor. This state of affairs leads us to conclude that faults in structure continuity are essential for the appearance of superconduction in the materials dealt with.

3 Superconducting electron pairs

A further point which is to be considered, in order to single out the right electron pairing mechanism, is the strong effect on critical temperature of some atomic substitutions shown by the superconducting compounds in Table 1. Indeed, partial substitution of Ba with K and of Pb with Bi between superconductors 2 and 3 originates an increase of T_c from 13 K to 30 K. Likewise, substitution of Ba with Sr between superconductors 3 and 4 decreases T_c from 30 K to 12 K. A similar effect is originated by the K to Rb substitution in the alkaly-stuffed fullerene, which increases T_c from 18 K to 28 K. This means that in these superconductors electrons are tightly coupled to the atoms present in the lattice structure. These electrons, therefore, can be conveniently represented by tight-binding (TB) wave functions, that is, linear combinations of atomic orbitals with appropriate wavy phase factors. Keeping in mind

that atomic orbitals with unpaired electrons tend to form spin-singlet bonds, the previous considerations induce us to argue that at low temperature electrons running in a region bordering on a lattice discontinuity originate bound pairs with electrons running in the region bordering on the opposite side of the lattice discontinuity. Bond stability depends on exchange integrals which, in turn, depend on Coulomb interactions of electrons with the lattice. Consequently, the electron-lattice interaction is shut up within the pairs, which are thus allowed to move freely through the lattice. Below are presented some simple equations dealing with this pairing mechanism.

Let us consider, within a lattice composed of ions of both signs, two regions a and b separated by a lattice discontinuity. By assuming that electrons moving in these regions interact mainly with ions of lattice vectors $\mathbf{u}_p$ and $\mathbf{v}_q$, respectively, their TB wave functions, ϕ_a and ϕ_b, can be written as

$$\phi_a(\mathbf{k}_a, \mathbf{r}_1) = \frac{1}{\sqrt{N}} \sum_{p=1}^{N} \mathrm{e}^{\mathrm{i}\mathbf{k}_a \cdot \mathbf{u}_p}\ a(\mathbf{r}_1 - \mathbf{u}_p),$$
$$\phi_b(\mathbf{k}_b, \mathbf{r}_2) = \frac{1}{\sqrt{N}} \sum_{q=1}^{N} \mathrm{e}^{\mathrm{i}\mathbf{k}_b \cdot \mathbf{v}_q}\ b(\mathbf{r}_2 - \mathbf{v}_q), \qquad (1)$$

$a(\mathbf{r}_1 - \mathbf{u}_p)$ and $b(\mathbf{r}_2 - \mathbf{v}_q)$ standing for the atomic orbitals and $\mathbf{k}_a$ and $\mathbf{k}_b$ for the electron wave vectors. The directions of $\mathbf{k}_a$ and $\mathbf{k}_b$ are obviously related to the geometry of a and b regions. With a layered geometry, $\mathbf{k}_a$ and $\mathbf{k}_b$ lie parallel to the layers. Normalization factors are determined by assuming that there is not much overlap between orbitals in neighbouring lattice positions. Energies of TB functions are given by the expectation values of Hamiltonians

$$\widehat{H}_a = \frac{\widehat{p}_1^2}{2m} - \sum_{p=1}^{N} \frac{Z_a\, e^2}{\mid \mathbf{r}_1 - \mathbf{u}_p \mid} + V_{\mathrm{lat}}(\mathbf{r}_1),$$
$$\widehat{H}_b = \frac{\widehat{p}_2^2}{2m} - \sum_{q=1}^{N} \frac{Z_b\, e^2}{\mid \mathbf{r}_2 - \mathbf{v}_q \mid} + V_{\mathrm{lat}}(\mathbf{r}_2), \qquad (2)$$

that is,

$$W_a(\mathbf{k}_a) = \langle \phi_a(\mathbf{k}_a, \mathbf{r}_1) \left| \widehat{H}_a \right| \phi_a(\mathbf{k}_a, \mathbf{r}_1) \rangle,$$
$$W_b(\mathbf{k}_b) = \langle \phi_b(\mathbf{k}_b, \mathbf{r}_2) \left| \widehat{H}_b \right| \phi_b(\mathbf{k}_b, \mathbf{r}_2) \rangle, \qquad (3)$$

$V_{\mathrm{lat}}(\mathbf{r})$ standing for the lattice potential due to ions in positions other than $\mathbf{u}_p$ and $\mathbf{v}_q$. On this ground, in analogy with the Heitler-London treatment of the hydrogen molecule [12] and disregarding the squared overlap integrals $\langle \phi_a \mid \phi_b \rangle$ of TB functions against unity, the pair wave function can be written as

$$\Psi(\mathbf{r}_1, \mathbf{r}_2) = \frac{1}{\sqrt{2}} [\phi_a(\mathbf{k}_a, \mathbf{r}_1)\phi_b(\mathbf{k}_b, \mathbf{r}_2) \pm \phi_a(\mathbf{k}_a, \mathbf{r}_2)\phi_b(\mathbf{k}_b, \mathbf{r}_1)] \begin{cases} S(1,2) \\ T(1,2) \end{cases} \qquad (4)$$

where plus or minus signs and $S\,(1,2)$ or $T(1,2)$ spin factors mean spin singlet or triplet states, respectively. The pair energy is given by the expectation value of the two-electron Hamiltonian

$$\widehat{H}_{a,\,b}(\mathbf{r}_1, \mathbf{r}_2) = -\sum_{q=1}^{N} \frac{Z_b\, e^2}{\mid \mathbf{r}_1 - \mathbf{v}_q \mid} - \sum_{p=1}^{N} \frac{Z_a\, e^2}{\mid \mathbf{r}_2 - \mathbf{u}_p \mid} + \frac{e^2}{r_{1,\,2}}\,. \qquad (5)$$

Therefore, by taking into account only the most significant exchange integrals, that is,

$$K_a = -\langle \phi_b(\mathbf{k}_b, \mathbf{r}_2) \mid \sum_{p=1}^{N} \frac{Z_a\, e^2}{\mid \mathbf{r}_2 - \mathbf{u}_p \mid} \mid \phi_a(\mathbf{k}_a, \mathbf{r}_2) \rangle,$$
$$K_b = -\langle \phi_a(\mathbf{k}_a, \mathbf{r}_1) \mid \sum_{q=1}^{N} \frac{Z_b\, e^2}{\mid \mathbf{r}_1 - \mathbf{v}_q \mid} \mid \phi_b(\mathbf{k}_b, \mathbf{r}_1) \rangle \qquad (6)$$

and

$$K'_{a,\,b} = \langle \phi_a(\mathbf{k}_a, \mathbf{r}_1)\phi_b(\mathbf{k}_b, \mathbf{r}_2) \mid \frac{e^2}{r_{1,\,2}} \mid \phi_a(\mathbf{k}_a, \mathbf{r}_2)\phi_b(\mathbf{k}_b, \mathbf{r}_1) \rangle, \qquad (7)$$

we have

$$W_{\mathrm{pair}} = \langle \phi_a(\mathbf{k}_a, \mathbf{r}_1)\, \phi_b(\mathbf{k}_b, \mathbf{r}_2) \mid \widehat{H}_{a,\,b}(1,\,2) \times \mid \phi_a(\mathbf{k}_a, \mathbf{r}_2)\phi_b(\mathbf{k}_b, \mathbf{r}_1) \rangle + \mathrm{h.c.}$$
$$= \pm\, \mathrm{Re}\, \left[\langle \phi_a \mid \phi_b \rangle K_a + \langle \phi_b \mid \phi_a \rangle K_b + K'_{a,\,b} \right]. \qquad (8)$$

Obviously, electron pairing occurs if W_{pair} is negative. Pairing energy is essentially an exchange or resonance energy. Its actual value depends on the distance between a and b regions. But also the electron momenta play a role. We point out, in this connection, that TB functions, neglecting a slight modulation like that of Bloch functions, can be approximated by plane waves. In fact, by taking into account that orbitals $a(\mathbf{r}_1 - \mathbf{u}_p)$ are closely localized at the lattice positions $\mathbf{u}_p$, only those orbitals for which $\mathbf{u}_p \simeq \mathbf{r}_1$ give a significant contribution in the sum of equation (1). Therefore, by letting such orbitals lie in the interval $p' \leq p \leq p''$, by putting $\mathbf{r}_1 - \mathbf{u}_p = \boldsymbol{\epsilon}_p$ and by considering that $\mid \boldsymbol{\epsilon}_p \mid \ll \mid \mathbf{r}_1 \mid$, we get

$$\phi_a(\mathbf{k}_a, \mathbf{r}_1) = \left[\frac{1}{\sqrt{N}} \sum_{p=p'}^{p=p''} a(\boldsymbol{\epsilon}_p) \right] \mathrm{e}^{\mathrm{i}\mathbf{k}_a \cdot \mathbf{r}_1}, \qquad (9)$$

where the factor in brackets is nearly constant. Consequently

$$\langle \phi_a \mid \phi_b \rangle \propto \delta_{\mathbf{k}_a, \mathbf{k}_b}, \qquad (10)$$

which, owing to equation (8), means that only electrons with alike $\mathbf{k}$, that is, alike momenta, allow for significant pairing energies. In the following, for simplicity, we restrict ourselves to this case.

It is clear that the pairs considered here have nothing to do with the Cooper's pairs which concern electrons with

opposite momenta. On the contrary, some likeness exists with the nucleon-nucleon pairs in nuclear matter. Actually, the nuclear forces, after separation of a self-consistent part, leave a residual interaction between nucleons which is rather weak, but which plays an important role in various nuclear properties. This residual interaction is essentially an exchange interaction owing to the peculiar nature of nuclear forces (Majorana forces). It couples nucleons with like momenta but with opposite projections of angular momenta along the quantization axis. Therefore, by dropping the boldface types, the coupled nuclear states can be marked with the indexes: k_1+, k_2-, instead of $-k, +k$ as the Cooper's pairs. An exhaustive treatment of pairing correlations in nuclear matter was performed by Belyaev [13] on the basis of the BV transformation[1]. This treatment can be directly applied to the electron pairs dealt with provided that components $\sigma = +$ and $\sigma = -$ of angular momentum are reinterpreted as the labels a and b of the neighbouring lattice regions[2]. This trick is allowed by the merely formal character of the BV transformation which leaves the physical nature of the pairs out of consideration. Therefore, by performing the substitution $k\,a, k\,b \Rightarrow k\,\sigma$ and by taking into account equation (8), we get, in line with reference [13]

$$W_{\text{pair}} \Rightarrow \langle k_1\,\sigma_1\,k_2\,\sigma_2 \mid G \mid k_2'\,\sigma_2'\,k_1'\,\sigma_1'\rangle\,. \tag{11}$$

In this way, with the substitutions $W_a(\mathbf{k}_a), W_b(\mathbf{k}_b) \Rightarrow \varepsilon_k$, the Hamiltonian of the interacting electron system can be written as

$$H = \sum_k (\varepsilon_k - \mu)\,(c_{k+}^+ c_{k+} + c_{k-}^+ c_{k-}) - \frac{1}{2}\sum_{k\sigma}\langle k_1\sigma_1 k_2\sigma_2 \mid G \mid k_2'\sigma_2' k_1'\sigma_1'\rangle\, c_{k_1\sigma_1}^+ c_{k_2\sigma_2}^+ c_{k_2'\sigma_2'} c_{k_1'\sigma_1'}, \tag{12}$$

μ standing for the chemical potential and $c_{k\,\sigma}^+$, $c_{k\,\sigma}$ for the fermion creation and destruction operators, respectively. Assuming $U_k^2 + V_k^2 = 1$ and inserting the transformation

$$c_{k+} = U_k\alpha_k + V_k\beta_k^+, \qquad c_{k-} = U_k\beta_k - V_k\alpha_k^+ \tag{13}$$

in equation (12), coefficient U_k and V_k can be determined by the diagonalizing condition

$$\sum_k \left[(\widetilde{\varepsilon}_k - \mu)\,2U_kV_k - \Delta_k(U_k^2 - V_k^2)\right](\alpha_k^+\beta_k^+ + \beta_k\alpha_k) = 0, \tag{14}$$

where

$$\Delta_k = \sum_{k_1}\langle k\ k \mid G \mid k_1k_1\rangle U_{k_1}V_{k_1} \tag{15}$$

and $\widetilde{\varepsilon}_k$ is the electron energy modified by the self-consistent field due to electron pairing interactions. In equation (15), matrix elements have the form

$$\langle k\ k \mid G \mid k_1k_1\rangle = \langle ka\ kb \mid G \mid k_1b\,k_1a\rangle - \langle ka\ kb \mid G \mid k_1a\,k_1b\rangle, \tag{16}$$

in which dependence on conjugated states a and b is shown explicitly. In this way, by taking into account diagonal terms $\alpha_k^+\alpha_k$ and $\beta_k^+\beta_k$ in the transformed Hamiltonian, the energy of quasi-particles is found to be

$$E_k = \sqrt{(\widetilde{\varepsilon}_k - \mu)^2 + \Delta_0^2}\,, \tag{17}$$

as in BCS theory. Likewise, by applying Fermi's statistic, the critical temperature law is obtained in the form

$$kT_{\text{c}} = 1.14\,\delta e \exp(-1/N_FV_0\,) \tag{18}$$

δe standing for the half-amplitude of the energy region around the Fermi level in which the matrix element (16) is different from zero, N_{F} for the density of states in this region and V_0 for the average value of element (16). With Cooper pairs, δe is related to Debye energy by $\delta e = \hbar\,\omega_{\text{D}}$ [16]. This result is a consequence of the fact that phonon coupling is active only for energies less than Debye energy. In general, for a system of weakly interacting fermions with attraction between particles other than phonon coupling, we have $2\,\delta e = \mu$ [17]. These results authorize the conclusion that the pairing mechanism dealt with leads to the appearance of an energy gap Δ_0 in the quasi-particles levels, as occurs with Cooper's pairs.

The different kinds of fermion pairs mentioned above are represented in Figure 1. Besides Cooper's pairs, Majorana's pairs are also shown, that is, nucleons coupled with identical linear momenta, but with opposite angular momenta. Electrons coupled in unconventional superconductors are also characterized by like linear momenta. Since these electrons lie in neighbouring lattice layers, the pairs are similar to the pairs of electrons lying in neighbouring atoms that were accounted for by Lewis in 1916 to explain molecular bonds. These pairs, therefore, can be referred to as Lewis's pairs [18].

4 Discussion

Arguments advanced thus far show how superconducting electron pairs may be originated in the materials dealt with. There is a wide variety of lattice structures, so that a special investigation is required for each material. We first consider YBCO cuprate which represents perhaps the most interesting case, owing to the great amount of pertinent experimental data now available.

4.1 The YBCO cuprate

The YBCO orthorhombic cell consists of three superimposed perovskitic cubes, the middle one containing

[1] An equivalent treatment of pairing correlations in nuclear matter was performed by Gor'kov [14] and Alekseev [15] utilizing the Green function technique.

[2] The sole difference between nuclear and superconductor treatments lies in the fact that for superconductors the preliminary separation of the self-consistent field due to the average particle interaction is unnecessary.

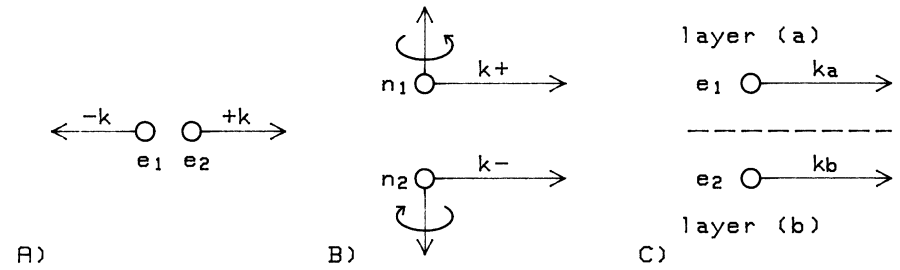

Fig. 1. Different kinds of pairs in fermion systems. A) in metallic solids electrons e_1 and e_2 with opposite linear momenta are coupled as Cooper's pairs. B) in nuclear matter nucleons n_1 and n_2 with like linear momenta but opposite angular momenta are coupled as Majorana's pairs. C) in unconventional superconductors electrons e_1 and e_2 running in neighbouring lattice layers are coupled with like linear momenta as Lewis's pairs.

yttrium at its center and the others barium. Divalent copper ions at the yttrium cube vertices are kept in lacunar oxygen octhaedra and lie on CuO_2 planes orthogonal to the c-axis. The oxygen lacunae are placed between divalent copper ions on edges of the yttrium cube parallel to the c-axis. Trivalent copper ions on the cell basal planes are separated alternately by oxygens and oxygen lacunae. With this symmetric geometry, regions a and b are identified with the CuO_2 planes facing each other at opposite sides of the yttrium cubes. Each copper ion in region b is separated from a corresponding ion in region a by length $\boldsymbol{\lambda}$ of the yttrium cube edges parallel to the c-axis, that is, $\mathbf{v}_q - \mathbf{u}_p = \boldsymbol{\lambda}$. Consequently, considering TB wave functions normalized as in equations (1) and taking into account that only nearest orbitals allow for significant overlap integrals, we obtain

$$\langle \phi_a \mid \phi_b \rangle = \frac{1}{N} \mathrm{e}^{\mathrm{i}\mathbf{k}\cdot\boldsymbol{\lambda}} \sum_{p=1}^{N} \int a(\mathbf{r}_1 - \mathbf{u}_p)\, b(\mathbf{r}_1 - \mathbf{u}_p - \boldsymbol{\lambda}) \mathrm{d}^3\mathbf{r}_1 = \mathrm{e}^{\mathrm{i}\mathbf{k}\cdot\boldsymbol{\lambda}} S_{a,b}, \tag{19}$$

where

$$S_{a,b} = \int a(\boldsymbol{\rho})\, b(\boldsymbol{\rho} - \boldsymbol{\lambda})\, \mathrm{d}^3\boldsymbol{\rho}. \tag{20}$$

As for exchange integrals, we have analogously

$$K_a = -\frac{1}{N} \mathrm{e}^{-\mathrm{i}\mathbf{k}\cdot\boldsymbol{\lambda}} \times \sum_{l=1}^{N} \int a(\mathbf{r}_2 - \mathbf{u}_l) \frac{Z_a\, e^2}{\mid \mathbf{r}_2 - \mathbf{u}_l \mid} b(\mathbf{r}_2 - \mathbf{u}_l - \boldsymbol{\lambda}) \mathrm{d}^3\mathbf{r}_2 = \mathrm{e}^{-\mathrm{i}\,\mathbf{k}\cdot\boldsymbol{\lambda}} E_{b,a} \tag{21}$$

where

$$E_{b,a} = -\int a(\boldsymbol{\rho}) \frac{Z_a\, e^2}{\mid \boldsymbol{\rho} \mid} b(\boldsymbol{\rho} - \boldsymbol{\lambda}) \mathrm{d}^3\boldsymbol{\rho}\,. \tag{22}$$

It is easy to see that, with the same approximation, the exchange integral $K'_{a,b}$ is vanishingly small. We have in fact

$$K'_{a,b} = \frac{1}{N^2} \sum_{p=1}^{N} \sum_{h=1}^{N} \int\int a(\mathbf{r}_1 - \mathbf{u}_p) b(\mathbf{r}_1 - \mathbf{u}_p - \boldsymbol{\lambda}) \times \frac{e^2}{r_{1,2}} a(\mathbf{r}_2 - \mathbf{u}_h) b(\mathbf{r}_2 - \mathbf{u}_h - \boldsymbol{\lambda}) \mathrm{d}^3\mathbf{r}_1 \mathrm{d}^3\mathbf{r}_2 = O\left(\frac{1}{N}\right), \tag{23}$$

since significant contributions arise only when $\mathbf{r}_1 \simeq \mathbf{r}_2$ and this in turn entails $\mathbf{u}_p \simeq \mathbf{u}_h$ so that the sums on p and h are coupled. Eventually, taking into account that $Z_a = Z_b$, it follows from equation (8)

$$W_{\mathrm{pair}} = 2\, S_{a,b}\, E_{b,a} \tag{24}$$

which, owing to the negative value of exchange integral $E_{b,a}$, corresponds to a singlet state. In this way, the W_{pair} found is independent of $\mathbf{k}$ so it remains constant for the whole electron distribution. It can therefore be directly identified with V_0 in equation (18).

Orbitals involved in previous equations are $3d$ orbitals characterized by prominent lobes arranged symmetrically around the ion centers. It is to be considered, however, that the electron distribution of copper ions is warped by the electric field due to neighbouring oxygen ions. In equations (2), potential V_{lat} has been introduced to account for this field. Indeed, the lacunar oxygen octhaedra, that is, the pyramids CuO_5 of five oxygens closest to divalent copper ions, originate the electric field

$$\mathbf{F}_{\mathrm{lat}} = \frac{2e}{(L/2)^2} \boldsymbol{\tau}, \tag{25}$$

$\boldsymbol{\tau}$ standing for a unit vector parallel to the c-axis and directed from copper to the pyramid apex and $L = 3.9$ Å for the length of the barium cube edge, that is, twice the distance between copper and the pyramid apex. This field polarizes the electron distributions of a and b copper ions which are stretched toward each other, thus greatly enhancing overlap of a and b orbitals and, as a consequence, the values of $S_{a,b}$ and $E_{b,a}$ integrals. Nevertheless, owing to the large separation $\mid \boldsymbol{\lambda} \mid = 3.2$ Å of copper ions, pairing energy surely remains small with respect to current covalent bond energies.

Table 2. Binding energies of oxygen ions in the different sites of the YBCO cell originated by their Coulomb interactions with the neighbouring ions. Items "Pyramid apex" (1) and (2) mark oxygen sites with neighbourhoods of Cu ions of different charges. Distance of oxygen from neighbouring Cu ions is $L/2$, from O^{-2}, Ba^{+2} and Y^{+3} ions is $L/\sqrt{2}$.

Oxygen ion site	Cell base	Pyramid apex (1)	Pyramid apex (2)	Pyramid base
Neighbouring ions	Cu^{+2}; Cu^{+3} 4 O^{-2}; 4 Ba^{+2}	2 Cu^{+2} 6 O^{-2}; 4 Ba^{+2}	Cu^{+2}; Cu^{+3} 6 O^{-2}; 4 Ba^{+2}	2 Cu^{+2} 6 O^{-2}; 2 Ba^{+2}; 2 Y^{+3}
Energy	$-20e^2/L$	$-(16-8\sqrt{2})e^2/L$	$-(20-8\sqrt{2})e^2/L$	$-(16-4\sqrt{2})e^2/L$
eV	−73.8	−17.8	−32.1	−38.2

Concerning the comparison of these results with experiments, the most significant observations are perhaps the large effects on critical temperature of pressure and oxygen content. Actually, various data on $\mathrm{d}T_\mathrm{c}/\mathrm{d}P$ have been reported. In particular, with fully-oxidized samples and with various substitutions on barium and yttrium, a value $\mathrm{d}T_\mathrm{c}/\mathrm{d}P = 0.96$ K/GPa was found for pressures up to 0.6 GPa [19,20]. As for the oxygen content, compounds of stoichiometry $YBa_2Cu^{II}_{2+2x}Cu^{III}_{1-2x}O_{7-x}$ with $x < 0.2$ show $T_\mathrm{c} = 92$ K, a figure that decreases to 60 K for $x \simeq 0.4$ [21]. To analyze these effects, it is useful to write equation (18) in differential form. Taking into account that $2\,\delta e = \mu$ [17], we have

$$\frac{\delta\, T_\mathrm{c}}{T_\mathrm{c}} = \log\left(\frac{0.57\,\mu}{kT_\mathrm{c}}\right)\frac{\delta V_0}{V_0}, \tag{26}$$

in which the logarithmic factor is positive since, as follows from equation (18), kT_c is exponentially small compared with μ, On the basis of this equation, the effect of pressure is readily understood. In fact, owing to the presence of oxygen lacunae, pressure easily reduces distance $\boldsymbol{\lambda}$ between the CuO_2 planes thus enhancing overlap and exchange integrals $S_{a,b}$ and $E_{b,a}$. This in turn allows for a larger $W_{\mathrm{pair},}$ that is, V_0 and, according to equation (26), for an increased T_c.

The effect of the oxygen content requires more attentive consideration. When an oxygen is removed, two trivalent copper ions are reduced to divalent and a further oxygen lacuna is introduced into the cell. To determine the position of this lacuna, binding energies of oxygen ions in the different sites of YBCO cell are to be compared. Three kinds of sites have to be considered, that is, sites on the cell bases and sites on the CuO_5 pyramid apices and bases, respectively. Owing to the essentially ionic character of the YBCO lattice, these energies are originated by Coulomb interactions of oxygen with neighbouring ions. In Table 2, oxygen binding energies are reported as evaluated by considering the nearest neighbouring ions and by assuming that on the cell bases divalent copper alternates with trivalent copper. Moreover, for simplicity's sake, all edges of barium and yttrium perovskitic cubes are assumed to have the same length $L \simeq 3.9$ Å. It appears that oxygens at the cell bases are the most tightly bound, while oxygens at the pyramid apices show the least binding energy. This result remains unchanged if ions placed at increasing distances and different arrangements of Cu^{+2} and Cu^{+3} ions on the cell bases are considered. It merely depends on the presence of oxygen lacunae on the basal planes, which reduces Coulomb repulsion between oxygens, and on the binding energy of trivalent yttrium, which exceeds that of divalent barium. It follows that oxygen removal mostly takes place at the pyramid apex, thus leaving copper in a neighbourhood of four oxygens arranged in a square configuration[3]. With this configuration, the polarizing field $\mathbf{F}_\mathrm{lat}$ drops to zero, thus greatly reducing overlap of copper orbitals. Since two oxygens, out of the seven present in the fully oxidized cell, lie at the pyramid apexes, in compounds with $x \simeq 0.4$ about 20% of a or b copper ions are unpolarized so that the corresponding $S_{a,b}$ and $E_{b,a}$ integrals are substantially smaller. Neglecting these integrals allows us to replace equations (19, 21) with

$$\langle \phi_a \mid \phi_b \rangle \simeq 0.8\,\mathrm{e}^{\mathrm{i}\mathbf{k}\cdot\boldsymbol{\lambda}} S_{a,b}, \qquad K_a \simeq 0.8\,\mathrm{e}^{-\mathrm{i}\mathbf{k}\cdot\boldsymbol{\lambda}} E_{b,a}, \tag{27}$$

respectively. In this way, even if the logarithmic factor in equation (26) is not large with respect to unity, the observed decrease of T_c can be justified. We get, in fact, $\delta T_\mathrm{c}/T_\mathrm{c} \simeq \delta V_0/V_0 \equiv \delta W_\mathrm{pair}/W_\mathrm{pair} \simeq 0.8^2 - 1 = -0.36$, to be compared with the experimental result $\delta T_\mathrm{c}/T_\mathrm{c} = (60-92)/92 = -0.35$. In spite of its merely qualitative nature, the previous discussion can be regarded as a reasonable explanation of the effect of oxygen removal. The conclusion follows that in YBCO cuprate the oxygen doping increases the average overlap of copper orbitals thus increasing T_c. To complete this analysis, we point out that also the orthorhombic-tetragonal transition for $x \geq 0.5$ can be ascribed to the removal of apex oxygens. In fact, apex oxygen lacunae allow for higher binding energies of oxygens placed in the four sites of the cell basal planes surrounding the copper ions close to these lacunae. Consequently, oxygens are gathered around these coppers, thus breaking the laying out of oxygens and lacunae in basal planes, which is responsible for the orthorhombic symmetry.

[3] Mossbauer spectroscopy of ^{57}Fe-doped YBCO has shown that in the orthorhombic fully-oxidized phase Fe^{+4} ions substitute Cu ions both on the cell basal planes (sites Cu1) and on the yttrium cube vertices (sites Cu2). When oxygen is removed, Fe^{+3} ions are found both in Cu1 and Cu2 sites [22]. That is: oxygen removal affects iron independently of its position. This means that removal takes place at the pyramid apex which lies just half-way between the copper sites. Removal from cell base or from pyramid base would have different effects on iron in Cu1 and Cu2 sites.

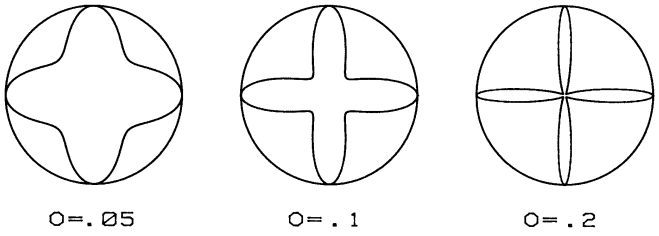

Fig. 2. Polar plots, for $\phi = \pi$ and different values of overlap integral O, of the superconducting energy gap as a function of angle θ between the electron wave vector $\mathbf{k}$ and the cell a-axis. The four maxima of the energy gap are lined up with a- and b-axes.

There is another question which deserves attention and which has long been debated in the last few years, that is, the question of the "s/d" symmetry of the order parameter. Different types of experiments have given conflicting data, so that a final conclusion has not been reached [23,24]. It is to be pointed out, however, that recent measurements by scanning tunnel microscopy on $Bi_2Sr_2CaCu_2O_{8+\delta}$ crystals containing zinc atom impurities have revealed the presence of four-fold symmetric quasi-particle clouds aligned with the Cu–O bonds on the CuO_2 planes [25,26]. This means that the superconducting energy gap is largest along the cell a- and b-axes. Such a result supports the d-symmetry option in cuprates. In the following, a simple argument is presented dealing with the symmetry of the energy gap in YBCO.

Owing to the orthorhombic but almost tetragonal symmetry of the YBCO cell, copper ions on the CuO_2 planes form a square grid with Cu^{+2} ions at the square vertices and O^{-2} ions at the middle of the square sides. The Coulomb field of O^{-2} ions cuts down the electron charge density of Cu^{+2} ions along the square sides, thus increasing density along the square diagonals. Consequently, the Cu^{+2} ion charge distribution becomes like that of $3d_{xy}$ orbitals[4]. By letting $\mathbf{u}_p$ and $\mathbf{u}_q$ be the lattice vectors and K a constant factor, normalization of TB wave functions yields

$$\langle \phi^*(\mathbf{k},\mathbf{r}) \mid \phi(\mathbf{k},\mathbf{r}\rangle = K^2 \left\langle \sum_{p=1}^{N} \mathrm{e}^{-\,\mathrm{i}\mathbf{k}\cdot\mathbf{u}_p} a(\mathbf{r}-\mathbf{u}_p) \mid \sum_{q=1}^{N} \mathrm{e}^{\mathrm{i}\mathbf{k}\cdot\mathbf{u}_q} a(\mathbf{r}-\mathbf{u}_q) \right\rangle = 1 \tag{28}$$

which leads to

$$K^2 = \left\{ N + 2 \sum_{q>\,p=1}^{N} \cos\left[\mathbf{k}\cdot(\mathbf{u_q}-\mathbf{u}_p)\right] O_{pq} \right\}^{-1}, \tag{29}$$

[4] Owing to the electric field $\mathbf{F}_{\mathrm{lat}}$, these orbitals are warped towards the YBCO cell centre, so that the electron charge distribution is not symmetrical with respect to the sides of the CuO_2 plane.

where

$$O_{pq} = \langle a(\mathbf{r}-\mathbf{u}_p) \mid a(\mathbf{r}-\mathbf{u}_q)\rangle \tag{30}$$

are the overlap integrals of Cu ion orbitals. The sum for $q > p$ in equation (29) includes $\binom{N}{2}$ terms. However, only the $2N$ terms with the minimum $\mathbf{u}_q - \mathbf{u}_p$ separation along the square diagonals give significant contributions. The terms along the square sides make no contribution owing to the presence of O^{-2} ions. By dropping labels p, q and putting

$$\mathbf{u}_q - \mathbf{u}_p = \boldsymbol{\delta}, \tag{31}$$

we have

$$K^2 = N^{-1} \left[1 + O \sum_{\vec{\delta}} \cos(\mathbf{k}\cdot\boldsymbol{\delta}) \right]^{-1}, \tag{32}$$

where $\mid \boldsymbol{\delta} \mid = \sqrt{2}L = 5.5$ Å. By assuming $\mathbf{I}$ parallel to the cell a-axis, taking into account that

$$\boldsymbol{\delta} = (\delta/\sqrt{2})(\pm\mathbf{I} \pm \mathbf{J}), \tag{33}$$

$$\mathbf{k} = k\cos\theta\,\mathbf{I} + k\sin\theta\,\mathbf{J} \tag{34}$$

and putting $K^2 N = \Phi(\theta)$, we obtain

$$\Phi(\theta) = \{1 + 2O\cos[\phi(\cos\theta + \sin\theta)] + 2O\cos[\phi(\cos\theta - \sin\theta)]\}^{-1} \tag{35}$$

where $\phi = k\delta/\sqrt{2}$ is a phase angle. In this equation, overlap integral O accounts for the electron charge distribution on the CuO_2 planes, while angle ϕ accounts for electron momenta. It follows that, when applying equations (8, 24), a further normalization factor $\Phi^2(\theta)$ is to be inserted in the expression of W_{pair}. Consequently, by letting the phase angle assume the value $\phi = k_{\mathrm{F}}\delta/\sqrt{2}$ at the Fermi level, the angular dependence of the superconducting energy gap is found to be

$$\Delta(\theta) \propto \Phi^2(\theta)\,\Delta_0. \tag{36}$$

This angular dependence corresponds to a four-fold symmetry. In fact, it can be seen from equation (35) that, while for $\phi = 0$, factor $\Phi^2(\theta)$ is independent of θ, for $\phi = \pi$ the ratios $\Phi^2(n\pi/4)/\Phi^2(0)$ $(n = 1, 2, 3, 4)$ are less than unity and attain a common minimum value. For intermediate values of ϕ, four-fold symmetry is still present, although less evident. It is interesting to note that for $\phi = \pi$, taking into account that $k_{\mathrm{F}} = 2\pi/\lambda_{\mathrm{F}}$, we have $\lambda_{\mathrm{F}}/2 = L$. Owing to the $3d_{xy}$ character of Cu ion orbitals, the maximun value of overlap integral is expected to be $1/4$. This occurs when one lobe out of four of each orbital is wholly overlapped with that of the other. When O tends to $1/4$, $\Phi^2(\theta)$ tends to infinity. Therefore, only values of O less than $1/4$ are significant. In Figure 2, $\Phi^2(\theta)$ is plotted for some values of O by assuming $\phi = \pi$.

The four-fold symmetry of the energy gap is evident. These results, although only of a qualitative nature, yield evidence in favour of *d*-symmetry.

Let us quote finally the following important experimental result which clearly substantiates the hypothesis that superconduction depends on interaction between the CuO_2 planes. Measurements of the Hall effect on YBCO single crystals have shown that the zero-temperature Ginzburg-Landau coherence length along the *c*-axis is about 1.5 Å. Since the spacing of superconducting layers is near the *c*-axis lattice parameter 11.68 Å this indicates that "*the two copper oxide planes, which are spaced* 3.2 Å, *are tightly coupled and act as a single superconducting layer*" [27].

4.2 The La_2CuO_4 cuprate

This compound consists of a stacking of $LaCuO_3$ perovskitic layers intercalated with LaO layers of the NaCl structure. The subsequent $LaCuO_3$ layers are displaced sidewise with respect to the stacking by half a perovskitic cube edge. With this geometry, regions *a* and *b* are identified with the copper ion planes lying at the sides of the LaO layers. Each copper ion in region *a* shows four nearest ions in region *b* with separations $\mathbf{v}_{p+n} - \mathbf{u}_p = \boldsymbol{\lambda}_{1+n} (n = 0, 1, 2, 3)$. Only these ions allow for significant contributions in overlap and exchange integrals. By proceeding as for equation (19), we thus have

$$\langle \phi_a \mid \phi_b \rangle = \sum_{n=0}^{4} \mathrm{e}^{\mathrm{i}\mathbf{k}\cdot\boldsymbol{\lambda}_{1+n}} S_{a,\,b}, \tag{37}$$

where

$$S_{a,\,b} = \int a(\boldsymbol{\rho})\, b(\boldsymbol{\rho} - \boldsymbol{\lambda}_1) \mathrm{d}^{\,3}\boldsymbol{\rho}, \tag{38}$$

since overlap integrals are independent of n owing to the square symmetry of separations $\boldsymbol{\lambda}_{1+n}$. Likewise, we have

$$K_a = \sum_{n=0}^{4} \mathrm{e}^{\mathrm{i}\mathbf{k}\cdot\boldsymbol{\lambda}_{1+n}} E_{a,\,b}, \tag{39}$$

where

$$E_{a,\,b} = -\int a(\boldsymbol{\rho}) \frac{Z_a\, e^2}{\mid \boldsymbol{\rho} \mid}\, b(\boldsymbol{\rho} - \boldsymbol{\lambda}_1) \mathrm{d}^{\,3}\boldsymbol{\rho}, \tag{40}$$

while, as in equation (23), integral $K'_{a,\,b}$ is negligible. In this way, by putting

$$\Theta(\mathbf{k}) = \sum_{n,m=0}^{4} \mathrm{e}^{\mathrm{i}\mathbf{k}\cdot(\boldsymbol{\lambda}_{1+n} - \boldsymbol{\lambda}_{1+m})} = 4 + 2\sum_{j=1}^{6} \cos(\mathbf{k}\cdot\boldsymbol{\sigma}_j) \tag{41}$$

where $\boldsymbol{\sigma}_j = \boldsymbol{\lambda}_{1+n} - \boldsymbol{\lambda}_{1+m}$ $(n \neq m)$ are the sides and the diagonals of the copper ion squares found at the bases of the $LaCuO_3$ cubes, we obtain

$$W_{\mathrm{pair}} = 2\,\Theta(\mathbf{k})\, S_{a,\,b}\, E_{b,\,a}. \tag{42}$$

As for equation (24), pairing energy is negative, but its actual value, which depends in this case on $\mathbf{k}$, is expected to be smaller than that for the YBCO cuprate owing to the larger Cu ion separations. This entails a smaller V_0 and, according to equation (26), a smaller critical temperature.

4.3 Perovskites

Perovskites with fractional stoichiometries are characterized by disordered lattices. Therefore, to identify the conjugated *a* and *b* regions, special hypotheses have to be introduced. Actually, all superconductors reported in Table 1, items 2 to 5, are constituted of $Me^{II}BiO_3$ (Me^{II} = Ba, Sr) cells, each holding an unpaired electron, embedded in $BaPbO_3$ or $Me^{I}BiO_3$ (Me^{I} = K, Rb) perovskitic lattices. We assume that the $Me^{II}BiO_3$ cells are joined in form of chains or layers. Two contiguous sets of joined cells are recognized as the conjugated regions. We assume, moreover, that the unpaired electrons are placed on the Me^{II} ions, so that Ba^{+1} or Sr^{+1} ions are found in the cells and the atomic orbitals appearing in the TB functions of equations (1) have to be identified with the *s*-orbitals of Ba or Sr atoms. As a consequence, separation $\boldsymbol{\lambda}$ of *a* and *b* orbitals equals the edge of the $Me^{II}BiO_3$ perovskitic cube. In this way, the notable variation of T_c originated by the substitution of barium with strontium in the $Ba_{0.6}K_{0.4}BiO_3$ compound (see Tab. 1) is at once understood. Indeed, the radius of the Sr^{+1} ion is smaller than that of the Ba^{+1} ion. Owing to the almost equal sizes of the Ba and Sr perovskitic cubes, the *s*-electron separation is larger with Sr^{+1} ions, thus reducing pairing energy and critical temperature from 30 K to 12-13 K. Similar considerations can be applied to the reduced strontium titanate $SrTiO_{3-\delta}$ as well (see Tab. 1 item 1).

4.4 Bechgaard salt

In Bechgaard salt, TMTSF molecules and $(TMTSF)^{+1}$ cations, together with $(PF_6)^{-1}$ anions, form stacks showing high metal-like conductivity parallel to the *a*-axis [10]. In directions transverse to the stackings, intermolecular coupling and conductivity are much smaller. Therefore, the conjugated *a* and *b* regions can be identified with contiguous stackings of these molecules. The geometry is, in some respect, similar to that of YBCO, but in equations (1) atomic orbitals should be substituted by the molecular orbitals of $(TMTSF)^{+1}$ cations. The unpaired electrons present in these cations originate intermolecular bonds between the conjugated regions. Pairing energy is expected to be rather weak, owing to the separation of the stackings. It is interesting to note that some anomalies observed with this material in connection with its magnetic behavior suggest the possibility of triplet pairing, instead of the usual singlet pairing [28].

4.5 Fullerene

As for the alkaly-stuffed fullerene, the interpretation is as follows. Sixty π-electrons are coupled in the C_{60} balls, thus originating thirty $\pi - \pi$ bonds, as occurs in the benzene molecule in which six π-electrons originate three $\pi - \pi$ bonds. In presence of the unpaired $3s$- or $4s$-electron of potassium or rubidium atom, one $\pi - \pi$ bond is broken, thus giving rise to a $3s$-π or $4s$-π bond between the C_{60} ball and the alkaly atoms and leaving an unpaired π-electron on the ball. The $Me^{I}C_{60}$ radicals thus originated can be assembled to form the conjugated regions. Lacking reliable data on the actual stacking of the C_{60} balls and the placing of the alkaly atoms, it seems risky to advance a more definite model of superconduction in this material. Despite this, fullerene is interesting since it provides clear evidence on the role of unpaired electrons in originating superconductivity.

5 Final remarks

In our opinion, the arguments advanced here yield considerable clues that the basic mechanism of electron pairing is essentially the same for all the unconventional superconductors considered above. The mechanism singled out relies on an electron exchange interaction showing a clear likeness with the ordinary exchange interaction that accounts for covalent bonds. In practice, the mechanism proposed can be regarded as a molecular mechanism in which the main feature is the coupling between electrons and atoms present in the lattice structure. It follows that the peculiarities of the Fermi surface are of little moment as regards the pairing mechanism. On the other hand, it should be taken into account that the superconductors dealt with range from perovskites to cuprates to organic compounds to fullerenes, which are quite dissimilar materials certainly characterized by different Fermi surfaces. Consequently, if the Fermi surface plays a significant role its variability would rule out the possibility of a pairing mechanism common to all superconductors.

To allow for a pairing mechanism fit for these diverse superconductors, the theoretical arguments herein advanced have been presented in a general way without reference to specific materials. For this reason, our treatment is a merely qualitative one. Actually, the atomic orbitals appearing in the TB wave functions (1) are undefined. With superconductors such as Bechgaard salt or fullerenes, molecular orbitals, that is, linear combinations of atomic orbitals, should be considered. To work out expectations relative to a particular superconductor, further theoretical arguments should be introduced. These would, however, require a quantitative treatment. Unfortunately, such treatment cannot be achieved by analytical methods, owing to the complexity of the matter dealt with. Actually, it would involve the development of onerous numerical calculations. In our opinion, this is out of place at the present time. To single out the proper mechanism, investigations of a general nature on superconduction phenomenology, also considering compounds with different transition metals[5], are probably still more advantageous.

It is to be pointed out that the superconduction mechanism we propose is quite different from that advanced by Anderson for YBCO cuprate [29]. In fact, the former ascribes superconduction to exchange interactions between electrons running in contiguous CuO_2 planes, while the latter appeals to superexchange interactions between copper ions mediated by oxygens in a network of –Cu–O–Cu– chains. Accordingly, each single CuO_2 plane shows superconduction. We note that, if this mechanism is taken into account, it becomes difficult to understand why monoclinic CuO, in which –Cu–O–Cu– chains are present as well, is not a superconductor.

In reality, the energy involved in the superconducting pairs is very weak. It is likely that, even in materials with the highest T_c, it attains at the most some tens of meV. Consequently, different mechanisms can be devised in principle, each sufficient to justify the pairing energy required. This is perhaps the main difficulty of the superconduction problem and explains why a large number of superconduction models have been proposed so far.

References

1. J. Ruvalds, Supercond. Sci. Technol. **9**, 905 (1996).
2. J. Bardeen, L.N. Cooper, J.R. Schrieffer, Phys. Rev. **108**, 1175 (1957).
3. N.N. Bogolyubov, JEPT USSR **34**, 58 and 73 (1958); Nuovo Cimento **7,** 794 (1958).
4. J.G. Valatin, Nuovo Cimento **7**, 843 (1958).
5. J.F. Schooley, W.R. Hosler, L. Cohen Marvin, Phys. Rev. Lett. **12**, 474 (1964).
6. A.W. Sleight, J.L. Gillson, P.E. Bierstedt, Solid State Comm. **17**, 27 (1975).
7. J.G. Bednorz, K.A. Muller, Z. Phys. B **64**, 189 (1986).
8. R.J. Cava, B. Batlogg, J.J. Kajewsky, R. Favrow, L.W. Rupp, A.E. White, K. Short, W.F. Pecks, T. Kometan, Nature **332**, 814 (1988).
9. S.M. Kazakov, C. Chaillout, P. Bordet, J.J. Capponi, M. Nunez-Regueiro, A. Rysak§, J.L. Tholence, P.G. Radaelli, S.N. Putilin, E.V. Antipov, Nature **390**, 148 (1997).
10. D. Jerome, in *Studies of High Temperature Superconductors*, Vol. **6**, 113 edited by A. Narkilar (Nova Science Publishers, New York, 1990).
11. M.J. Rosseinsky, A.P. Ramirez, S.H. Glarum, D.W. Murphy, R.C. Haddon, A.F. Hebard, T.T.M. Palstra, A.R. Kortan, S.M. Zaurak, A.V. Makhija, Phys. Rev. Lett. **66,** 2830 (1991).

[5] We point out, in this connection, that the monovalent mercury cation Hg^{+1} shows the electronic configuration $[Xe]\,6s^2 4f^{14} 5d^9$ with an unpaired electron in the d-subshell like divalent copper. Actually, monovalent mercury forms dimer cations $[Hg_2]^{+2}$, as occurs in the chloride Hg_2Cl_2 (calomel). This means that monovalent mercury possesses a special bent for originating electron pairs, a feature that might play a role in some high T_c superconductors.

12. L. Pauling, E.B. Wilson, *Introduction to Quantum Mechanics* (McGraw-Hill, New York, 1935) Ch. XII.
13. S.T. Belyaev, Mat. Fys. Medd. Dan. Vid. Selsk. **31**, No. 11 (1959); JEPT USSR **9**, 23 (1958).
14. L.P. Gor'kov, JEPT **7**, 505 (1958).
15. A.I. Alekseev, Soviet Phys. Usp. **4**, 1, 23 (1961).
16. G.D. Mahan, *Many-Particle Physics* (Plenum Press, New York, 1981), Ch. 9.
17. L.D. Landau, E.M. Lifshitz, *Statistical Physics* (Pergamon Press, Oxford, 1969), Ch. VII.
18. G.N. Lewis, J. A. C. S. **38**, 762 (1916).
19. J.J. Neumeier, M.B. Maple, M.S. Torikachvii, Physica C **156**, 574 (1988).
20. J.G. Huber, V.J. Liverman, Y. Xu, A.R. Moodenbaug, Phys. Rev. B **41**, 8757 (1990).
21. R.J. Cava, B. Batlogg, K.M. Rabe, E.A. Rietman, P.K. Gallagher, L.W. Rupp, Physica C **156,** 523 (1988).
22. R.A. Brand, Ch. Sauer, H. Lütgemeier, B. Rupp, W. Zinn, Physica C **156**, 539 (1988).
23. A. Barone, Il Nuovo Cimento D **16**, 1635 (1994).
24. R.A. Klemm, *High Temperature Superconductivity*, edited by K.B. Garg, S.M. Bose (Narosa Publishing House, New Delhi, 1998), p. 179.
25. A.V. Balatsky, Nature **403**, 717 (2000).
26. S.H. Pan, E.W. Hudson, K.M. Lang, H. Elsaki, S. Uchida, J.C. Davis, Nature **403**, 746 (2000).
27. J.P. Rice, J. Giapintzakis, D.M. Ginsberg, J.M. Mochel, Phys. Rev. B **44,** 10158 (1991).
28. I.J. Lee, M.J. Naughton, G.M. Danner, G.M. Chaikin, Phys. Rev. Lett. **78**, 3555 (1997).
29. P.W. Anderson, Phys. Rep. **184**, 195 (1989).